

Accepted Manuscript

Title: Development and supercapacitor application of ionic liquid-incorporated gel polymer electrolyte films

Authors: Ravi Muchakayala, Shenhua Song, Jingwei Wang, Youhua Fan, Manjunatha Benggeppagari, Jianjun Chen, Manlin Tan



PII: S1226-086X(17)30548-8
DOI: <https://doi.org/10.1016/j.jiec.2017.10.009>
Reference: JIEC 3665

To appear in:

Received date: 12-7-2017
Revised date: 26-9-2017
Accepted date: 1-10-2017

Please cite this article as: Ravi Muchakayala, Shenhua Song, Jingwei Wang, Youhua Fan, Manjunatha Benggeppagari, Chen Jianjun, Manlin Tan, Development and supercapacitor application of ionic liquid-incorporated gel polymer electrolyte films, Journal of Industrial and Engineering Chemistry <https://doi.org/10.1016/j.jiec.2017.10.009>

This is a PDF file of an unedited manuscript that has been accepted for publication. As a service to our customers we are providing this early version of the manuscript. The manuscript will undergo copyediting, typesetting, and review of the resulting proof before it is published in its final form. Please note that during the production process errors may be discovered which could affect the content, and all legal disclaimers that apply to the journal pertain.

Development and supercapacitor application of ionic liquid-incorporated gel polymer electrolyte films

Ravi Muchakayala^a, Shenhua Song^{a,*}, Jingwei Wang^a, Youhua Fan^a, Manjunatha Benggeppagari^b, Jianjun Chen^c, Manlin Tan^{c,**}

^a Shenzhen Key Laboratory of Advanced Materials, Shenzhen Graduate School, Harbin Institute of Technology, Shenzhen 518055, China.

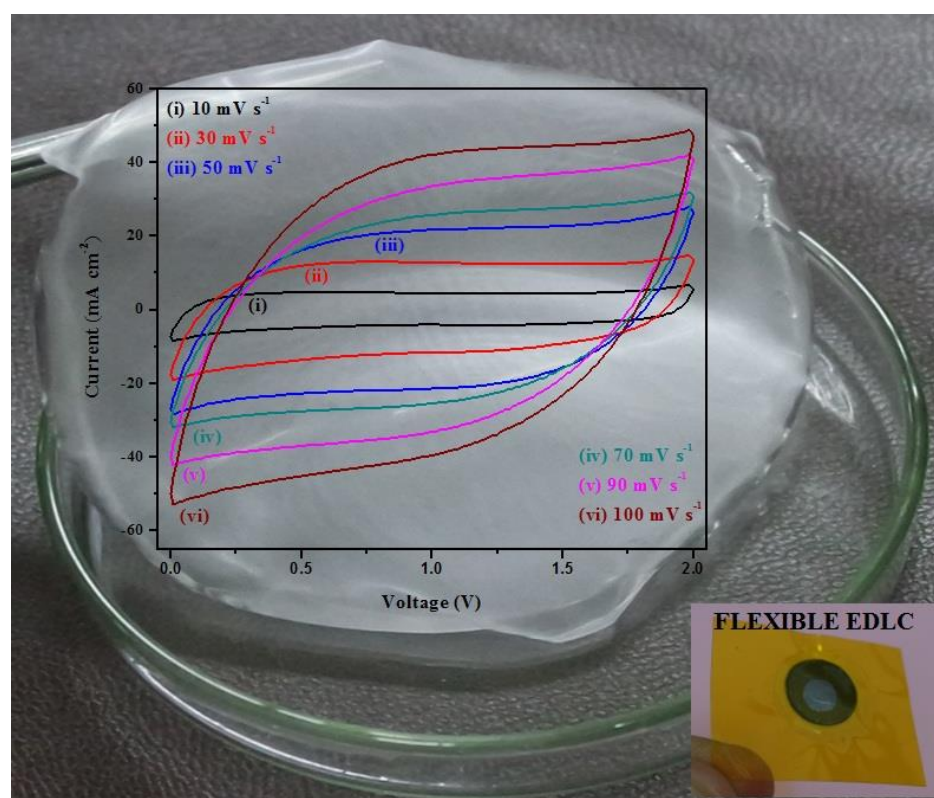
^b Center for Biofluid and Biomimic Research, Pohang University of Science and Technology (POSTECH), Pohang 790-784, South Korea.

^c Research Institute of Tsinghua University in Shenzhen, Shenzhen 518055, China.

* Corresponding author. Fax: +86-755-26033504. E-mail addresses: shsonguk@aliyun.com; shsong@hit.edu.cn (S. Song).

** Corresponding author. E-mail address: tanml@tsinghua-sz.org (M. Tan).

GRAPHICAL ABSTRACT



Research Highlights

- PVdF-HFP:[PMpyr][NTf₂] gel polymer electrolyte membranes are prepared.
- A high ionic conductivity of $1.59 \times 10^{-3} \text{ S cm}^{-1}$ is gained for 80 wt.% [PMpyr][NTf₂] membrane.
- The maximum C_{sp} is 156.64 F g^{-1} for MWCNT-added AC electrode-based EDLC.

Abstract

A new gel polymer electrolyte based on 1-methyl-1-propylpyrrolidinium bis(trifluoromethyl sulfonyl)imide ([PMpyr][NTf₂]) entrapped in poly(vinylidene fluoride-hexafluoropropylene) (PVdF-HFP) is prepared and optimized for flexible solid state supercapacitor applications. The structural, thermal, electrical and electrochemical properties of the ionic liquid gel polymer electrolyte membranes are studied by different characterization techniques. The transparent gel polymer electrolyte membranes exhibit high amorphicity and excellent thermal stability. The 20PVdF-HFP:80[PMpyr][NTf₂] gel polymer electrolyte membrane possesses a high ionic conductivity ($1.596 \times 10^{-3} \text{ S cm}^{-1}$) and wide electrochemical stability window (4.7 V) at room temperature. It is used as the electrolyte material for the fabrication of flexible electric double layer supercapacitors (EDLCs) with multiwalled carbon nanotube (MWCNT)-added and unadded activated carbon (AC) electrodes. The performances of flexible EDLCs are evaluated using cyclic voltammetry and galvanostatic charge-discharge measurements. The EDLC with MWCNT-added AC

electrodes exhibits apparently higher specific capacitance of electrode (156.64 F g^{-1}), specific energy (30.69 Wh kg^{-1}) and specific power (4.13 kW kg^{-1}) than that with AC electrodes. The cyclic stability of the former is still in a good condition at the 2000th charge-discharge cycle and much better than the latter. The present comparative study indicates that the 20PVdF-HFP:80[PMpyr][NTf₂] gel polymer electrolyte is a good candidate for the development of flexible solid-state supercapacitors.

Keywords: Gel polymer electrolyte films; Thermal stability; Electrical properties; Supercapacitors

1. Introduction

Recently, there has been an increasing demand for the flexible solid state energy storage devices and their technology because of their widespread electronic device applications in the modern society [1, 2]. The rechargeable batteries, fuel cells and electrochemical capacitors are currently used in energy conversion devices. Among these, the electrochemical capacitor is one of the potential energy storage devices, which possesses long cycling life ($\sim 10^5$ to 10^6), high specific power, high specific capacitance, moderate specific energy, fast charging and discharging, and operational safety [3, 4]. Electrochemical capacitor is also referred to as “supercapacitor” or ultracapacitor” because its specific capacitance is six orders of magnitude higher than that of conventional capacitors [5, 6]. Based on the charge storage mechanism and electrode materials, the electrochemical supercapacitors are divided into two categories, namely, electric double layer capacitors (EDLCs) and pseudo-capacitors.

In the EDLCs, charge storage is a purely electrostatic process and there is no faradic reaction occurring, i.e., electrostatic charges/ions are accumulated at the

electrode-electrolyte interface, which produces the resultant capacitance of the device. So the EDLCs exhibit high power density, fast charging–discharging and long cyclic stability but low energy density [7, 8]. A conventional supercapacitor (SC) is generally composed of two electrodes (active material coated on the collectors) with electrolyte and separator. The electrolyte works as a medium to transport ions between the electrodes and to avoid electric contacting between electrodes. Most of the reported EDLCs contain high specific surface area carbon as electrode, liquid electrolyte, and polymer membrane as separator. Liquid electrolyte-based supercapacitors have several drawbacks, such as liquid leakage, bulky size, corrosion with electrodes, self-discharge, low-temperature operation and hard to design in different shapes, which prevent their applications in different light weight and microelectronic devices. Hence, it is urgently needed to develop a new material (electrodes with suitable electrolyte) and its related technologies for the fabrication of flexible solid state electric double layer supercapacitors with consideration of environmentally safe and cost effective as well as device performance optimization. One of the best promising strategies for the development of flexible solid state electrochemical double layer supercapacitors is to replace the liquid electrolyte by the gel polymer electrolyte, which can reduce the size and weight of the device significantly by avoiding the strict sealing and holding requirements [9, 10]. This means that a flexible solid state electric double layer supercapacitor comprises a gel polymer electrolyte film between the two electrodes. So the flexible solid state EDLC device performance completely depends on both electrode and electrolyte materials.

More than 80% of researchers have been focusing their attention on electrode material development and EDLC performance testing. They concluded that the carbon materials, such as activated carbon, carbon nanotubes and graphene, worked as electrodes for the fabrication of EDLCs and exhibited good performances. Based on the reported results, in the present study the activated carbon (AC) and multiwalled carbon nanotubes (MWCNTs) were chosen as electrode materials for the EDLCs fabrication.

The gel polymer electrolyte is a crucial material in the flexible EDLCs. It serves as a separator between the two electrodes and also as a medium to transport ions between the electrodes. So the gel polymer electrolyte significantly influences the performances of EDLCs.

Most of the reported gel polymer electrolytes contain a salt solution in a polar organic solvent (e.g., propylene carbonate, ethylene carbonate, etc.) immobilized in a host polymer, such as poly(methyl methacrylate) (PMMA), polyacrylonitrile (PAN), poly(vinyl alcohol) (PVA) and poly(vinylidene fluoride-hexafluoropropylene) (PVdF-HFP) [11-14]. These gel polymer electrolytes are free standing films and possess high ionic conductivity, thermal and mechanical stabilities. However, their applicability is restricted in electrochemical device applications because of their low electrochemical stability range, volatile and flammable nature. To overcome these problems, ionic liquid incorporated gel polymer electrolytes have been recently developed for supercapacitor applications. The ionic liquid works as plasticizer and releases ions for conduction, and also it is non-volatile and non-flammable with

excellent electrochemical stability. From the available research reports, 1-methyl-1-propylpyrrolidinium bis(trifluoromethyl sulfonyl)imide ([PMpyr][NTf₂]) shows excellent electrical and electrochemical properties. Trigueiro et al. [15] studied the thermal, electrical and electrochemical properties of [PMpyr][NTf₂] ionic liquid and compared their results with those from other ionic liquids, demonstrating that this ionic liquid works as a good electrolyte material because it exhibits better properties than the others [16-18]. Gonzalez et al. [19] also investigated the physical properties of [PMpyr][NTf₂] in detail and concluded that it was a good electrolyte material at both room temperature and high temperatures. Hence, in the present study, the [PMpyr][NTf₂] ionic liquid was chosen for the preparation of gel polymer electrolyte films. Until the present time, few research publications have been available for flexible solid state double layer supercapacitors based on ionic liquid gel polymer electrolytes [20, 21]. Therefore, it is a novel research area with scientific importance in the modern society for the further development of electronic industrial sectors.

The main aim of the present study is to improve the electric double layer capacitor performances by using ionic liquid gel polymer electrolytes. For achieving this, we have done this work as two parts. Firstly, we developed ionic liquid incorporated PVdF-HFP gel polymer electrolyte films and optimized their properties for the requirement of flexible solid-state electric double layer capacitors. Secondly, flexible supercapacitors were fabricated by using optimized gel polymer electrolyte films with suitable electrode materials and their performances were evaluated. Undoubtedly, this is a new research area and the findings will give some useful information for the

further development of the electronic industrial sector in the modern society.

2. Experimental details

2.1. Preparation and characterization of ionic liquid-modified gel polymer electrolytes

Ionic liquid incorporated gel polymer electrolyte films were developed by solution casting. Poly(vinylidene fluoride-hexafluoropropylene) (PVdF-HFP, $M_w = 400000$) was dissolved in tetrahydrofuran (THF, analytical grade) by magnetic stirring at 50 °C for 2 h to obtain a transparent solution. Simultaneously, the predetermined weight of the 1-methyl-1-propylpyrrolidinium bis(trifluoromethyl sulfonyl)imide ([PMpyr][NTf₂]) were separately dissolved in THF by magnetic stirring for 1 h at room temperature in 50, 60, 70, and 80 wt.%. The [PMpyr][NTf₂] ionic liquid solution was mixed with the PVdF-HFP solution and the mixture was continuously stirred for 12 h at room temperature to yield a homogeneous solution. Finally, the mixed solution was cast into clean glass petri dishes and the THF solvent was evaporated slowly at ambient temperature to form a gel polymer electrolyte films on the bottoms of the dishes. The obtained gel polymer electrolyte films were kept in a vacuum oven at 60 °C for 24 h to remove residual solvent and moisture. In the obtained PVdF-HFP:[PMpyr][NTf₂] ionic liquid gel polymer electrolyte films, the [PMpyr][NTf₂] ionic liquid releases ions for conduction, and the host polymer PVdF-HFP provided mechanical stability for ionic conduction through polymer chain entanglements. After adding more than 80 wt.% [PMpyr][NTf₂] ionic liquid, the gel polymer electrolyte films were like smooth paste and their physical nature was not stable enough for EDLC device fabrication, implying that when the [PMpyr][NTf₂]

ionic liquid concentration was beyond 80 wt.%, the host PVdF-HFP could not provide the mechanical stability of the films because its content was too low. The photomicrograph of the 20PVdF-HFP:80[PMpyr][NTf₂] gel polymer electrolyte film is shown in Fig. 1. Obviously, the film is free-standing and suitable for the fabrication of EDLCs. Similar types of gel films were also obtained by some other researchers [22, 23]. The film thickness was determined to be approximately 120 μm by means of a micrometer.

X-ray diffraction (XRD) is an effective technique of examining the structural characteristic of materials and their changes with the addition of dopants. The XRD patterns of the host PVdF-HFP polymer and [PMpyr][NTf₂] ionic liquid incorporated PVdF-HFP gel polymer electrolyte films were recorded using a D/max Rigaku X-ray diffractometer with Cu K α radiation ($\lambda = 1.5406 \text{ \AA}$) at a scanning rate of 2° per min. The applied accelerating voltage and current were kept 40 kV and 30 mA, respectively. When the ionic device (supercapacitor or battery) operates continuously, its temperature automatically increases. Consequently, the gel polymer electrolyte films must exhibit a good thermal stability for their practical applications. The thermal events and stability of the gel polymer films were examined by a STA 449F3 Jupiter thermal analyzer over the temperature range of 30–650 $^\circ\text{C}$ at a heating rate of 10 $^\circ\text{C}$ per min. For supercapacitor applications, the electrical and electrochemical properties of a gel polymer electrolyte film play a crucial role. Hence, the ionic conductivity values of the gel polymer electrolyte films were measured by a computer-interfaced impedance analyzer (PSM 1735, Newton 4th Ltd, UK) in the

frequency range 1 Hz - 1 MHz at room temperature. The working voltage range of the gel polymer electrolyte film was evaluated by using an electrochemical analyzer (CHI 766 F, CH Instrument, China) in the cyclic voltammetry (CV) mode. In both electrical and electrochemical measurements, the gel polymer electrolyte films were cut into circular pieces and sandwiched between a pair of stainless steel foil with a symmetrical cell configuration (SS/electrolyte/SS; electrode cross-section area = 0.785 cm²).

2.2. Preparation of electrodes

Commercially available activated carbon (AC, supercapacitor grade), acetylene black (AB), PVDF and N-methyl-2-pyrrolidone (NMP) were procured from TMC and used as received. The flexible graphite sheet with a thickness of 250 μm was purchased from Sigma-Aldrich and used as the current collector. In the preparation of EDLC electrodes, the different materials AC, AB and PVDF were taken in mortar in a weight ratio 80:10:10 and thoroughly mixed to obtain a composite powder. NMP solvent was added into the composite powder and the mixture was then magnetically stirred for 10 hours to gain a homogeneous slurry. This slurry was uniformly cast onto the flexible graphite sheet by using doctor blade instrument and dried overnight at 100 °C, becoming an AC electrode. In these electrodes, the activated carbon acts as the active material, the acetylene black as the conductivity enhancer or conductive additive, and the PVDF as the polymeric binder. Furthermore, it is worth noting that the conductive additive has manifold advantages, i.e., it acts as electron-transfer catalyst, substrate for current leads, and agent to control porosity and

surface area, etc.

Multiwalled carbon nanotubes (MWCNTs) (thickness = 1-10 graphene layers) were purchased from Sigma-Aldrich and used as received. The purity of the MWCNTs is important as it influences the device performance. Hence, their structural characteristics were examined by XRD and transmission electron microscopy (TEM, FEI Tecnai G2 F30), which are represented in Fig. 2. Obviously, they are typical MWCNTs without visible impurities.

For the preparation of supercapacitor electrode, the component materials AC, MWCNT, AB, and binder PVDF were taken in the weight ratio of 40:40:10:10 and thoroughly mixed in a mortar for 5 h to acquire composite powders. NMP is added into the composite powders and then the mixture was ultrasonicated for 2 h, and further magnetically stirred for 12 h to harvest a fine/smooth paste. This paste was also coated on the flexible graphite sheet and dried at 100 °C, becoming an MWCNT-added AC electrode. Both the MWCNT added and unadded AC electrodes were cut into circular shape and stored in a protective glow box. These circular shaped electrodes were directly used for fabrication of EDLCs. The average thickness of the electrode was about 100 μm and the average mass loading was 0.005 g.

Owing to the fact that the surface area and porosity of electrode materials are crucially important for the development of high performance supercapacitors, the specific surface area and porosity of AC were evaluated using a surface analyzer (ASAP 2020, USA). The obtained values were that BET surface area = 1893.56 m^2/g , pore volume = 1.035 cm^3/g and average particle size = 31.68 nm. These values are

well comparable with the reported ones [24, 25].

2.3. Fabrication and characterization of flexible EDLC cells

Flexible EDLC cells were assembled with the as-prepared gel polymer electrolyte films and symmetrical electrodes. One piece of gel polymer electrolyte film was placed between two symmetrical electrodes (electrode cross-section area = 0.937 cm^2) and then pressed tightly for good electrode-electrolyte contact. The entire cell was sealed with a self-assembled plastic pouch, which contains special contact arrangement for device performance measurements. These cells have significant advantages, such as no leakage, small thickness and good flexibility, making them suitable for small scale electronic device applications. The schematic diagram of an EDLC is shown in Fig. 3 along with an assembled EDLC supercapacitor. As can be seen, the prepared EDLC has two identical electrodes and thus it is named as the symmetrical EDLC. In this study, two types of EDLCs were assembled and their configurations are given below:

Cell I: AC electrode/20PVdF-HFP:80[PMpyr][NTf₂] gel polymer electrolyte/AC electrode; Cell II: MWCNT-added AC electrode/20PVdF-HFP:80[PMpyr][NTf₂] gel polymer electrolyte/ MWCNT-added AC electrode. The performance of flexible EDLCs was evaluated using cyclic voltammetry (CV), electrochemical impedance spectroscopy (EIS) and galvanostatic charge-discharge (GCD) cycling with the aid of an electrochemical workstation (Model 608C, CH Instrument). The EIS measurements of solid-state EDCLs were conducted in the frequency range of 100 kHz to 1 MHz at room temperature. The cyclic voltammetry responses of the EDCLs

were measured at different scan rates over the potential range of 0 to 2 V. In addition, the galvanostatic charge-discharge characteristics of the EDCLs were also recorded over the potential range of 0 to 2 V at room temperature.

3. Results and discussion

3.1. Analysis and optimization of gel polymer electrolyte films

3.1.1 Structural analysis

Fig. 4 shows the XRD patterns of pristine PVdF-HFP and PVdF-HFP:[PMpyr][NTf₂] gel polymer electrolyte films with various contents of [PMpyr][NTf₂]. The structural features of the pristine PVdF-HFP have been clearly discussed in our previous reports [26, 27]. As known from the reported results, the pristine PVdF-HFP film exhibits a semi-crystalline structure i.e., it contains both crystalline and amorphous parts. As can be seen from Fig. 4, after the addition of 50 wt.% [PMpyr][NTf₂] ionic liquid in the pristine PVdF-HFP, there are significant changes in XRD patterns: some peaks vanish, all crystalline peaks are broadened and their intensities are decreased, indicating that the [PMpyr][NTf₂] ionic liquid and PVdF-HFP polymer matrix are mixed in the molecular level. With further increasing [PMpyr][NTf₂] content, the crystalline peak intensities slightly decrease and their widths increase. This may be due to the disruption of PVdF-HFP crystalline structure by the [PMpyr][NTf₂] ionic liquid. The addition of [PMpyr][NTf₂] ionic liquid can reduce the intermolecular interaction of PVdF-HFP polymer chains, thereby increasing the amorphous region.

From the XRD patterns, the degree of crystallinity can be evaluated [28]. The degree of crystallinity of a polymer may be calculated by the following

equation $\chi_c = (A_c/A_t) \times 100$, where A_c is the area under the crystalline peaks and A_t is the total area under the XRD curves. The calculated degree of crystallinity of pristine PVdF-HFP is 45.8 %, which decreases with increasing [PMpyr][NTf₂] content and reaches a small value of 17.5 % for the 80 wt.% [PMpyr][NTf₂] film. This implies that the 20PVdF-HFP:80[PMpyr][NTf₂] gel polymer electrolyte membrane exhibits a high amorphous nature. Similar XRD features were also observed by other researchers in the polymer electrolytes incorporated with different ionic liquids [29, 30].

The high amorphous nature is a prerequisite for achieving a high ionic conductivity for a gel polymer electrolyte. According to Ratner et al. [31], the ionic conduction of the gel polymer electrolyte membranes occurs in the amorphous phase. In the amorphous phase, the polymer chains are more flexible, increasing the ionic mobility and thereby enhancing the ionic conductivity of the system. Hence, it is anticipated that the 20 PVdF-HFP:80[PMpyr][NTf₂] gel polymer electrolyte system may exhibit a high ionic conductivity. Furthermore, there are no additional peaks present in the gel polymer electrolyte systems, implying that the materials involved in the electrolyte system are highly compatible and homogeneous.

3.1.2 Thermal analysis

TGA curves of pristine PVdF-HFP, 50PVdF-HFP:50[PMpyr][NTf₂] and 20PVdF-HFP:80[PMpyr][NTf₂] polymer films are represented in Fig 5. The TGA curve of the pristine PVdF-HFP polymer film is an almost straight line and does not show any weight loss until 430 °C, indicating that the pristine PVdF-HFP is thermally stable. The major weight loss of 80.55% occurs at 430 °C due to the decomposition of

PVdF-HFP polymer chains. With the addition of 50 wt.% [PMpyr][NTf₂] ionic liquid, the thermal stability of the gel polymer electrolyte significantly deteriorates, i.e., the thermal degradation start temperature shifts to a lower temperature of 389 °C. When the [PMpyr][NTf₂] concentration is increased from 50 to 80 wt.%, the thermal degradation start temperature further shifts to a lower temperature of 384 °C, which could be due to the disruption of the polymer structure by the ionic liquid. When the [PMpyr][NTf₂] ionic liquid is incorporated into the host PVdF-HFP polymer, it will disrupt the PVdF-HFP crystalline structure and then the disrupted polymer matrix will melt at a lower temperature, leading to a lower degradation start temperature. Nevertheless, the thermal stability of the 20PVdF-HFP:80[PMpyr][NTf₂] gel polymer electrolyte is quite high enough for supercapacitor applications. Similar behavior was also observed by other researchers [24, 32, 33]

3.1.3 Conductivity analysis

In flexible EDLCs, the gel polymer membrane works as electrolyte and separator, i.e., it separates the two electrodes and provides ions for conduction between the electrodes. So the ionic conductivity of the gel polymer electrolyte membrane is a crucial parameter for flexible supercapacitors and it significantly influences the device performance. Based on the impedance measurements at room temperature, the values of ionic conductivity for different electrolyte films were obtained, which are represented in Fig. 6. As can be seen, the ionic conductivity increases with increasing [PMpyr][NTf₂] concentration and the 20PVdF-HFP:80[PMpyr][NTf₂] gel polymer electrolyte exhibits a high ionic conductivity of approximately $1.6 \times 10^{-3} \text{ S cm}^{-1}$.

Several researchers [33, 34-37] also studied PVdF-HFP-based gel polymer electrolytes. The maximum room-temperature ionic conductivity was obtained as $1.68 \times 10^{-4} \text{ S cm}^{-1}$ for PVdF-HFP + DMOImTf [34], $1.4 \times 10^{-4} \text{ S cm}^{-1}$ for 1PVdF-HFP:2EMIBF₄, $6.0 \times 10^{-5} \text{ S cm}^{-1}$ for 1PVdF-HFP:2EMIPF₆ and $2.2 \times 10^{-3} \text{ S cm}^{-1}$ for 1PVdF-HFP: 2EMITf [35], $5.0 \times 10^{-5} \text{ S cm}^{-1}$ for 20PVdF-HFP :80(LiTFSI/PyR14TFSI) , and $8.0 \times 10^{-5} \text{ S cm}^{-1}$ for 20PVdF-HFP:80(LiTFSI/Py24TFSI) [36], $1.7 \times 10^{-4} \text{ S cm}^{-1}$ for 10PVdF-HFP:EMIM-TFSA/LiTFSI and $1.04 \times 10^{-4} \text{ S cm}^{-1}$ for 10PVdF-HFP:MPPYrrTFSA/LiTFSI [37], and $2.0 \times 10^{-3} \text{ S cm}^{-1}$ for 4PVdF-HFP:1EMImFAP [33]. Obviously, the present ionic conductivity ($1.6 \times 10^{-3} \text{ S cm}^{-1}$) is well comparable with the previously reported ones. This ionic conductivity should be high enough for practical applications.

The above experimental phenomenon can be explained according to the general conductivity equation [38] $\sigma = n_i q_i \mu_i$, where n_i is the density of mobile charge carriers, q_i is the charge of the carrier and μ_i is the mobility of mobile charge carriers. From this relation, the enhancement in the ionic conductivity of gel polymer electrolytes can be achieved by increasing n_i and μ_i (q_i is the same for all charge carriers). When the 50 wt.% [PMpyr][NTf₂] ionic liquid is added into the host PVdF-HFP polymer matrix, a large number of mobile ions will be created in the system, which is mainly responsible for the increase in ionic conductivity. In addition, the [PMpyr][NTf₂] ionic liquid can also improve the amorphous nature of the host polymer, i.e., the ionic liquid or ions can interact with the host polymer and reduce the

intermolecular interaction between the polymer chains, thereby increasing the amorphicity of the system. Within the amorphous phase, the mobile charge carriers have a high mobility and the segmental motion of polymer chains is enhanced. This is also responsible for the increase in ionic conductivity. In addition, the high amorphous nature of the 20PVdF-HFP:80[PMpyr][NTf₂] gel polymer electrolyte film may enable the film to have a good contact with the electrodes. This is important for fabrication of flexible EDLCs because the energy storage arises from the ion accumulation at the electrode-electrolyte interface.

3.1.4 Electrochemical stability window analysis

The cyclic voltammetry (CV) curves of [PMpyr][NTf₂] ionic liquid incorporated gel polymer electrolyte films were recorded at ambient temperature for the evaluation of electrochemical stability window which indicate the working voltage range of gel polymer electrolyte films. It is an important parameter to quantify the usefulness/applicability of gel polymer electrolytes in the flexible electrochemical supercapacitor. Fig. 7 shows the typical cyclic voltammograms of PVdF-HFP + x [PMpyr][NTf₂] gel polymer electrolyte films ($x = 50, 60, 70$ and 80 wt.%) at a scan rate of 10 mV s^{-1} . As can be seen, the electrochemical stability window of the 50PVdF-HFP:50[PMpyr][NTf₂] electrolyte film is in the range $-2 \text{ V} - 2 \text{ V}$ (i.e., 4.0 V), indicating that in this region no chemical reaction can occur between the electrolyte and electrode. With increasing [PMpyr][NTf₂] concentration from 50 to 80 wt.%, an increase in electrochemical stability window is observed (see in Fig. 7). The 20PVdF-HFP:80[PMpyr][NTf₂] gel polymer electrolyte exhibits a wide

electrochemical stability window, ranging from -2.4 V to 2.3 V, i.e., 4.7 V, which may be due to its high ionic conductivity as well as high amorphous nature. This electrochemical potential window is high enough for the development of advanced flexible supercapacitors. As shown above, the 20PVdF-HFP:80[PMpyr][NTf₂] gel polymer electrolyte membrane possesses good structural, thermal, electrical and electrochemical properties. Hence, this membrane was used as electrolyte and separator for fabrication of advanced flexible supercapacitors.

3.2. Flexible solid-state EDLC device performance

The EDLC device performance and its electrochemical behavior at the electrode-electrolyte interface were analyzed using three different experimental techniques: cyclic voltammetry (CV) and galvanostatic charge-discharge cycling (GCD). All these measurements were conducted on the EDCL cells (Cell-I and Cell-II) based on the 20PVdF-HFP:80 [PMpyr][NTf₂] electrolyte film.

3.2.1 Cyclic voltammetry analysis of flexible EDLC cell

Charge storage mechanism at the electrode-electrolyte interface and switching behavior of flexible supercapacitor cells were examined by cyclic voltammetry studies. Fig. 8a shows the comparative cyclic voltammetry responses of flexible EDLC cells (Cell -I and Cell-II) between 0 to 2 V at a scan rate 10 mV s⁻¹. The CV curves of EDLC cells are almost rectangular-shaped, which indicates that the major capacitive storage mechanism is the electric double layer supercapacitor, i.e., two capacitive layers are formed at the electrode-electrolyte interface [24, 39].

Furthermore, in both CV curves (i.e., Cell-I and Cell-II) no redox peaks are present,

indicating that non-faradic reaction takes place in the EDLC, i.e., the energy storage in the EDLC is mainly due to ion accumulation at the electrode-electrolyte surface. The 20PVdF-HFP:80[PMpyr][NTf₂] gel polymer electrolyte has a large number of mobile charge carriers, they drift to electrodes and adsorb on the surfaces of pores then the charge accumulation is formed at the electrode-electrolyte interface. This charge accumulation is well known as the electric double layer on each electrode of the device. When the voltage is applied across the cell, the energy can be stored inside the EDLC. It is clear from Fig. 8a that Cell-II exhibits a more rectangular shape CV curve with higher voltammetric currents. This may be due to a better contact/compatibility between MWCNT-added AC electrode and gel polymer electrolyte film. The specific capacitance of electrode (C_{sp}) is calculated from CV curves by [40]

$$C_{sp} = \frac{A}{mSV} \quad (1)$$

where A is the area outlined by the CV curve, m is the mass of electrode, s is the scan rate, and V is the potential window (2 V in the present case).

The calculated specific capacitance of electrode is 158.39 F g⁻¹ for Cell-II and 95.01 F g⁻¹ for Cell-I. The higher specific capacitance of the MWCNT-added AC electrode-based supercapacitor (Cell-II) is due to its better pore structure. The MWCNT-added AC electrode material has a good pore structure and thus a large number of ions/charge carriers are accumulated at the electrode-electrolyte interface and their mobility is also increased, which is responsible for the higher specific capacitance. Moreover, the good electrode-electrolyte contact is another cause for the

higher specific capacitance of Cell-II. The MWCNT-added electrode has a lower resistance with the gel polymer electrolyte film at the interface so that the mobile charge carriers require a lower energy to overcome this resistance. Consequently, the mobile charge carriers are more easily adsorbed on the electrode surface and form the electric double layer which leads to an increase in the specific capacitance of the EDLC device. The observed specific capacitance values are comparable with the reported ones [20, 24]. Besides, it may be noted that the specific capacitance of the 20PVdF-HFP:80[PMpyr][NTf₂] gel polymer electrolyte-based EDLC cell can be improved by selecting a more suitable electrode material. For instance, the MWCNT-added AC electrode is better than the AC electrode.

Cyclic voltammetry responses with different scan rates are represented in Fig. 8b and c. It is evident that the CV response of Cell-I is rectangular-shaped only at a lower scan rate and a significant change occurs at a scan rate of 100 mV s⁻¹. This may be because there is a higher internal resistance in the system. The deviation in the CV responses of supercapacitor cell is associated with the high resistive components in the real capacitors [41]. For Cell-II, the CV responses are almost rectangular-shaped within the studied scan rate range, indicating that there is a good electric double layer at the electrolyte-electrolyte interface.

The specific capacitance values of both EDLCs are plotted in Fig. 8d as a function of scan rate. It shows that the specific capacitance drops considerably with increasing scan rate until 30 mV s⁻¹, and decreases slightly with further increasing scan rate. This behavior is generally observed by carbon-based EDLCs due to the

resistance for bigger charge carriers to pass through the pore structure of active materials. It should be noted that Cell-II has a higher specific capacitance and less fading percentage at any scan rate than Cell-I. This could be due to the proper electric double layer formation and faster switching behavior of charge carriers at the electrode-electrolyte interface in Cell-II. The MWCNT-added AC electrode material has a better pore structure than the AC electrode material. This may enable the electrode-electrolyte interface to have a better contact in Cell-II so that more charge carriers can be accumulated at the electrode-electrolyte interface, leading to a higher specific capacitance with less fading. Accordingly, the 20PVdF-HFP:80[PMpyr][NTf₂] gel polymer electrolyte film is more compatible with the MWCNT-added electrode than with the unadded one.

Electrochemical impedance spectroscopy (EIS) is a versatile characterization technique to understand the electrode-electrolyte interface behavior of EDLCs. Fig. 9 shows the Nyquist impedance plots of the EDLC cells at ambient temperature, measured in the frequency range 1 Hz - 1 MHz. It is seen that both plots consist of a semicircle in the high frequency range and an inclined spike in the low frequency range, indicating its double layer capacitive behavior. This is generally observed in porous carbon electrode-based supercapacitors [42, 43]. As shown, there are two resistive (R_b and R_{ct}) components, which are determined from the semicircle intercepts on the real axis. The high-frequency intercept is associated with the bulk resistance (R_b) of the gel polymer electrolyte membrane, which is constant because both EDLCs have a common 20PVdF-HFP:80[PMpyr][NTf₂] gel polymer electrolyte

membrane. The low-frequency intercept gives the combination of charge transfer resistance (R_{ct}) and bulk resistance (R_b). The charge transfer resistance is related to the electrode-electrolyte interface, including the ionic and electronic resistances in the EDLCs. The ionic resistance is the resistance encountered by charge carriers (ions), which is significantly influenced by the pore structure of electrodes. The electronic resistance arises from electrode particles and contact between active electrode layer and graphite current collector. The electronic resistance is negligible because the electrode material contains electronic conductor and the graphite current collector is highly electronic-conducting. Hence, the charge transfer resistance results mainly from the ionic resistance. The Nyquist plot of Cell-I shows a bigger semicircle than Cell-II. This reflects that Cell-I has some ion transport limitations at the electrode-electrolyte interface and thus it has a high interface resistance. However in the case of Cell-II, the MWCNT works as channels for ion transport and therefore it has a lower interface resistance. The charge transfer resistances of Cell-I and Cell-II are 40.14 and 30.14 ohms, respectively, confirming that the MWCNT-added AC electrode has a better compatibility with the gel polymer electrolyte membrane. These results are in good accordance with the CV analysis. The lower charge transfer resistance of Cell-II should be due to the pore structure of the MWCNT-added AC electrode. A small charge transfer resistance can significantly enhance the performance of EDLCs.

The equivalent circuit analysis of EDLC Nyquist plots may provide clear information about interface properties. The proposed equivalent circuit (modified

Randle's circuit) of EDCL Nyquist plot is shown as an inset in Fig. 9. In this circuit, the parameter R_b represents the combined effect of the bulk resistance of the electrolyte and the internal resistance of the electrode, which appears in the high frequency region. The parallel combination of charge transfer resistance R_{ct} and double-layer capacitance C_{dl} emerges in the high to mid frequency region. The linear region of the 45° slope is attributed to the Warburg impedance element (W) related to the ion diffusion resistance arising from ion diffusion through porous electrodes [24, 44]. This Warburg impedance (W) can be expressed as $A/(j\omega)^n$, where A is called the Warburg coefficient, ω is the angular frequency, and n is an exponent, which is a correction factor (varying from 0 to 1) associated with the roughness of the electrode [45]. The capacitive element (C_L) is associated with the capacitance at the electrode-electrolyte interface, which is observed in the low frequency range.

3.2.2 Galvanostatic charge–discharge analysis

Cyclic voltammetry is not enough to completely understand the electrochemical properties of EDLCs. Hence, the galvanostatic charge–discharge (GCD) performances of EDLCs are examined. Fig. 10 a shows the charge-discharge profiles of Cell-I and Cell-II in the first cycle at a constant current density of 5 mA cm^{-2} . Both of the cells exhibit almost a linear discharge characteristic, which further confirms the superior capacitive nature of the EDLCs.

In the charge-discharge profile, an initial voltage sudden jump/drop during charging/discharging is present, which is due to the ohmic loss coming from the internal resistance between gel polymer electrolyte membrane and electrode [46]. It is

also referred to as equivalent series resistance (ESR) of the EDLCs, being calculated from the initial voltage drop in the discharge profile.

The capacitance of the EDLCs (C_{cell}) is calculated from the discharge curve by

$$C_{\text{cell}} = \frac{i \cdot \Delta t}{\Delta V} \quad (2)$$

where i is the constant current, Δt is the discharge time, ΔV is the voltage drop during discharging in time Δt .

The specific capacitance of electrode (C_{sp}) is given by

$$C_{\text{sp}} = 2C_{\text{cell}}/m \quad (3)$$

The specific capacitances of cell-II and cell-I in the first cycle are 156.64 F g⁻¹ and 93.72 F g⁻¹, respectively, i.e., Cell-II exhibits a higher specific capacitance than Cell-I, which is in good agreement with the CV results. Specific capacitances of electrode for some gel polymer electrolyte membrane-based solid state supercapacitors are listed in Table 1 for comparison. It is clear that the specific capacitance of 20PVdF-HFP:80[PMpyr][NTf₂] gel polymer electrolyte membrane-based supercapacitors are well comparable with the reported ones [21,24,39,41,43,47].

The specific energy (E) and specific power (P) of each EDLC cell are calculated by [30]

$$E = \frac{1}{2m} C_{\text{cell}} \Delta V^2 \quad (4)$$

$$P = \frac{\Delta V^2}{4m \cdot ESR} \quad (5)$$

where ESR is the equivalent series resistance. The ESR value is evaluated from the

GCD curve by [20]

$$ESR = \frac{\Delta V_{iR}}{2i} \quad (6)$$

where ΔV_{iR} is the ohmic drop of the device. The obtained *ESR* values are 34.4 and 32.0 Ohms for Cell-I and Cell-II, respectively. These values are acceptable and comparable with the reported ones [44, 48]. The low *ESR* value is an indication of high contact or low barrier for ion transport between the polymer electrolyte and electrode. Hence the lower the *ESR*, the better the EDLC system. A low *ESR* value may be obtained if one is careful in the electrolyte and electrode preparation and device fabrication, thereby leading to a small ohmic drop ΔV_{iR} . The specific capacitance of electrode, specific energy, and specific power values of each EDLC in first charge–discharge cycle are listed in Table 2. As can be seen, Cell-II exhibits much higher specific energy and specific power than Cell-I, indicating that the MWCNT-added AC electrode-based EDLC exhibits better performances because the electrode possesses a better pore structure along with a better contact/compactability between MWCNT-added AC electrode and gel polymer electrolyte membrane.

The cyclic stability performance of the carbon-based EDLCs is one of the important aspects and it is examined by extended charge-discharge cycles at a constant current density of 5 mA cm⁻² in the voltage range of 0 - 2 V, which are shown in Fig. 10b and c. The specific capacitances of EDLC cells as a function of cyclic number are represented in Fig. 10d. As shown, the specific capacitance decreases in the few cycles and then it maintains almost constant until 2000 cycles. The decrease in specific capacitance is due to the charge depletion layer formation and the increase

in internal resistance. At the beginning of charge-discharge, few mobile charge carriers are blocked in the porous structure of electrode and thus a depletion layer on the electrode-electrolyte interface or electrode surface is formed. Hence, the number of mobile charge carriers is reduced and the internal resistance also increases with increasing cyclic number. This should be responsible for the initial fading of specific capacitance. It should be noted that the specific capacitance of Cell-II is 116.88 F g^{-1} after 2000 cycles, i.e., there is just a 25% decrease, but it is 54% for Cell-I. It should be noted that the specific capacitance of Cell-II is 116.88 F g^{-1} after 2000 cycles, i.e., there is just a 25% decrease, but it is 54% for Cell-I. This means, after 2000 cycles the maximum specific capacity retention (cyclic stability) is 75 % for MWCNT added-AC electrode and 48% for pure AC electrode. The observed cyclic stability values are a little bit poor compared to others. Generally, the cyclic stability of the device is influenced by numbers of factors such as electrolyte and electrode properties and device fabrication processes. In the present supercapacitor systems, the $[\text{PMpyr}]^+$ and $[\text{NTf}_2]^-$ are transport ions, which have bigger radius so that some of these ions may be blocked in the porous electrode during the charging and discharging process. These blocked ions can produce a repulsive force to the same ions in the next charging-discharging cycle. As a result, the cyclic stability of the device may reduce with the number of cycles. From the GCD results, we noticed that the MWCNT-added AC electrode supercapacitor with the 20PVdF-HFP: 80[PMpyr][NTf₂] gel polymer electrolyte exhibits an excellent cyclic stability. The performance of the 20 PVdF-HFP:80[PMpyr][NTf₂] gel polymer electrolyte-based EDCL device can be

improved by selecting suitable electrode materials.

4. Conclusions

Flexible and free-standing gel polymer electrolyte films based on [PMpyr][NTf₂] ionic liquid entrapped in the PVdF-HFP matrix are prepared and characterized. The structural and thermal studies confirm that the 20 PVdF-HFP:80[PMpyr][NTf₂] system exhibits high amorphicity and good thermal stability. It also possesses a high ionic conductivity ($1.596 \times 10^{-3} \text{ S cm}^{-1}$) and a wide electrochemical stability window (4.7 V). The 20PVdF-HFP:80[PMpyr][NTf₂] gel polymer electrolyte-based EDLCs with two types of electrode materials (AC electrode and MWCNT-added AC electrode) are fabricated and their performances are evaluated using cyclic voltammetry and galvanostatic charge-discharge cycling. Compared with the AC electrode-based EDLCs, the MWCNT-added AC electrode-based EDLCs show apparently higher specific capacitance of electrode, specific energy and specific power, being up to 156.64 F g^{-1} , 30.69 Wh kg^{-1} and 4.13 kW kg^{-1} in the first cycle, respectively. It also exhibits an excellent cyclic stability up to 2000 cycles. These studies indicate that the 20PVdF-HFP:80[PMpyr][NTf₂] gel polymer electrolyte-based EDLC device with the MWCNT-added AC electrode performs excellently, implying that this gel polymer electrolyte is a promising candidate for the development of flexible supercapacitors.

Acknowledgments: This work was supported by the Science, Technology and Innovation Commission of Shenzhen Municipality (Grant No. JCYJ20160301100700645) and the Science & Technology Department of Guangdong

Province (Grant No. 2016B020244001).

References

1. Huisheng Peng, Xuemei Sun, Wei Weng, Xin Fang, Flexible electronic Devices based on polymers, *Polymer Materials for Energy and Electronic Applications*, 9 (2017) 325-354.
2. Minghao Yu, Teng Zhai, Xihong Lu, Xiaojun Chen, Shilei Xie, Wei Li, Chaolun Liang, Wenxia Zhao, Liping Zhang, Yexiang Tong, Manganese dioxide nanorod arrays on carbon fabric for flexible solid-state supercapacitors, *Journal of Power Sources* 239 (2013) 64-67.
3. Ander Gonzalez, Eider Goikolea, Jon Andoni Barrena, Roman Mysyk, Review on supercapacitors: Technologies and materials, *Renewable and Sustainable Energy Reviews* 58 (2016) 1189-1206.
4. Minghao Yu, Xinyu Cheng, Yinxiang Zeng, Zilong Wang, Yexiang Tong, Xihong Lu and Shihe Yang, Dual-Doped Molybdenum Trioxide Nanowires: A Bifunctional Anode for Fiber-Shaped Asymmetric Supercapacitors and Microbial Fuel Cells, *Angew. Chem. Int. Ed.* 55(2016) 6762-6766.
5. Minghao Yu, Dun Lin, Haobin Feng, Yinxiang Zeng, Yexiang Tong and Xihong Lu, Boosting the Energy Density of Carbon-Based Aqueous Supercapacitors by Optimizing the Surface Charge, *Angew. Chem. Int. Ed.* 56 (2017) 5454-5459.
6. Minghao Yu, Shaobin Zhao, Haobin Feng, Le Hu, Xiyue Zhang, Yinxiang Zeng, yexiang Tong, Xihong Lu, Engineering Thin MoS₂ Nano-sheets on TiN Nanorods: Advanced Electrochemical capacitor Electrode and Hydrogen Evolution Electrocatalyst, *ACS Energy Letters* 2 (2017) 1862-1868.

7. Hye-Min Lee, Hong-Gun Kim, Shin-Jae Kang, Soo-Jin Park, Key-Hyeok An, Byung-Joo Kim, Effects of pore structures on electrochemical behaviours of polyacrylonitrile (PAN) based activated carbon nanofibers, *Journal of Industrial and Engineering Chemistry* 21 (2015) 736-740.
8. B. E. Conway, *Electrochemical Supercapacitor: Scientific Fundamentals and Technological Applications*, Kluwer Academic/Plenum, New York 1999.
9. Cheng Zhong, Yida Deng, Wenbin Hu, Jinli Qiao, Lei Zhang and Jiujun Zhang, A review of electrolyte materials and compositions for electrochemical supercapacitors, *Chem. Soc. Rev.*, 44 (2015) 7484-7539.
10. Minghao Yu, Yi Han Xinyu cheng, Le Hu, Yinxiang Zeng, Meiqiong Chen, Faliang Cheng, Xihong Lu and Yexiang Tong, Holey Tungsten Oxynitride Nanowires: Novel Anodes Efficiently Integrate Microbial Chemical Energy Conversion and Electrochemical Energy Storage, *Advanced Materials* 27 (19) (2015) 3085-3091.
11. A.M.M. Ali, M.Z.A. Yahya, H. Bahron, R.H.Y. Subban, M.K. Harun, I. Atan, Impedance studies on plasticized PMMA-LiX (X: CF₃SO₃, N(CF₃SO₂)₂⁻) polymer electrolytes, *Materials Letters* 10 (2007) 2026-2029,
12. L.N. Sim, F.C. Sentanin, A.Pawlicka, R. yahya, A.K. Arof, Development of polyacrylonitrile-base polymer electrolytes incorporated with lithium bis(trifluoromethane) sulfonamide for application in electrochromic device, *Electrochimica Acta* 229 (2017) 22-30,
13. D. Vinoth Pandi, S. Selvasekarapandian, R. Bhuvaneswari, M. Premalatha, S. Monisha, D. Arunkumar, kawamura Junichi, Development and characterization of

- proton conducting polymer electrolyte based on PVA, amino acid glycine and NH_4SCN , *Solid State Ionics* 298 (2016) 15-22,
14. Ki-Sub Kim, Seul Bee Lee, Hyunjoo Lee, Hoo Sik Kim, Youngwoo Lee, Kwangsoo Kwack, Poly(vinylidene fluoride)-hexafluoropropylene-methyl N-methylpyrrolidinium-N-acetate trifluoromethanesulfonylimide-lithium trifluoromethanesulfonylimide gel electrolytes, *Journal of Industrial and Engineering Chemistry* 15 (5) (2009) 657-660.
15. Joao Paulo C. Trigueiro, Rodrigo L. Lavall, Glaucia G.Silva, Supercapacitors based on modified graphene electrodes with poly(ionic liquid), *Journal of Power Sources* 256 (2014) 264-273.
16. K.K.Denshchikov, M.Y.Izmaylova, A.Z. Zhuk, Y. S. Vygodskii, V.T. Novikov, A.F. Gerasimov, *Electrochimica Acta* 55 (2010) 7506-7510.
17. A. Balducci, R. Dugas, P.L. Taberna, P. Simon, D.Plee, M. Mastragostino, S. Passerini, *Journal of Power Sources* 165 ((2007) 922-927.
18. R.S. Borges, H. Ribeiro, R.L. Lavall, G.G.Silva, *J. Solid State Electrochemi.* 16(2012)3573-3580.
19. Begone Gonzalez, Emilio Gonzalez, Physical properties of the pure 1-methyl-1-propylpyrrolidinium bis(trifluoromethylsulfonyl)imide ionic liquid and its binary mixtures with alcohols, *J. Chem. Thermodynamics* 68(2014) 109-1163.
20. Gai P. Pandey, Tao Liu, Cody Hancock, Yonghui Li, Xiuzhi Susan Sun, Jun Li, Thermostable gel polymer electrolyte based on Succinonitrile and ionic liquid for high performance solid state supercapacitors, *Journal of Power Sources*, 328 (2016)

510-519.

21. P. Tamilarasan, S. Ramaprabhu, Grapheme based all-solid state supercapacitors with ionic liquid incorporated polyacrylonitrile electrolyte, *Energy* 51 (2013) 374-381.

22. PeiXia Yang, Lei Liu, LiBo Li, Jun Hou, Yan Ping Xu, Xuefeng Ren, Mao Zhong An, Ning Li, Gel polymer electrolyte based on polyvinylidene fluoride-co-hexafluoro propylene and ionic liquid for lithium ion battery, *Electrochimica Acta* 115 (2014) 454-460.

23. Safna Hussan K. P, Mohamed Shahin Thayyil, S.K. Deshpande, Jinita T.V., Jayant Kolte, Development of ion conducting ionic liquid-based gel polymer electrolyte membrane PMMA/BMPyr.TFSI-with improved electrical, optical, thermal and structural properties, *Solid State Ionics* 310 (2017) 166-175.

24. G.P. Pandey, S.A. Hashmi, Solid-state supercapacitors with ionic liquid based gel polymer electrolyte: Effect of lithium salt addition, *Journal of Power Sources* 243 (2013) 211-218.

25. Shu Ye, Lei Zhu, Ick-Jun Kim, Sun-hye Yang, Won-Chun Oh, Characterization of expanded graphene nanosheet as additional material and improved performance for electric double layer capacitors, *Journal of Industrial and Engineering Chemistry* 43 (2016) 53-60.

26. Xin Tang, Ravi Muchakayala, Shenhua Song, Zhongyi Zhang, Anji Reddy Polu, A study of structural, electrical and electrochemical properties of PVdF-HFP gel polymer electrolyte films for magnesium ion battery applications, *Journal of*

- Industrial and Engineering Chemistry 37 (2016) 67-74,
27. Jiwu Tang, Ravi Muchakayala, Shenhua Song, Meng Wang, Naveen Kumar, Effect of EMIMBF₄ ionic liquid addition on the structure and ionic conductivity of LiBF₄ complexed PVdF-HFP polymer electrolyte films, Polymer Testing 50 (2016) 247-254.
28. M. Ravi, Shenhua Song, Jingwei Wang, Ting Wang, Reddeppa Nadimicherla, Ionic liquid incorporated biodegradable gel polymer electrolyte for lithium ion battery applications , J. Materials Science and Materials Electronics 27 (2016) 1370-1377.
29. Yogesh Kumar, S.A. Hashmi, G.P. Pandey, Ionic liquid mediated magnesium ion conducting in poly(ethylene oxide)based polymer electrolyte, Electrochimica Acta 56(2011) 3864-3873.
30. Mohd.Suleman, Yogesh Kumar, S.A. Hashmi, Solid state electrical double layer capacitors fabricated with plastic crystal based flexible gel polymer electrolytes: Effective role of electrolyte anions, Materials Chemistry and Physics 163(2015)161-171.
31. M.A. Ratner, D.F. Shriver, Ion Transport in Solvent-Free polymers, Chem. Rev 88 (1988) 109-124,
32. Mohd. Suleman, Yogesh Kumar, S.A. Hashmi, Structural and Electrochemical properties of Succinonitrile-based gel polymer electrolytes: Role of ionic liquid addition, The Journal of Physical Chemistry 117 (2013) 7436-7443.
33. G. P. Pandey, S.A. Hashmi, Performance of solid state supercapacitors with ionic liquid 1-ethyl-3-methylimidazolium tris(pentafluoroethyl) trifluorophosphate based

gel polymer electrolyte and modified MWCNT electrodes, *Electrochimica Acta* 105 (2013) 333-341.

34. Boor Singh, S.S. Sekhon, Ion conducting behavior of polymer electrolytes containing ionic liquids, *Chemical Physics Letters* 414 (1-3) (2005) 34-39.

35. Joan Fuller, Amy C. Breda, Richard T. Carlin, Ionic Liquid-polymer gel electrolytes from hydrophilic and hydrophobic ionic liquids, *Journal of Electroanalytical Chemistry* 459 (1998) 29-34.

36. Jagth Pitawala, Maria Assunta Navarra, Bruno Scrosati, Per Jacobsson, Aleksandar Matic, Structure and properties of Li-ion conducting polymer gel electrolytes based on ionic liquids of the pyrrolidinium cation and the bis(trifluoromethanesulfonyl)imide anion, *Journal of Power Sources* 245 (2014) 830-835;

37. Andreas Hofmann, Michael Schulz, Thomas Hanemann, Gel electrolytes based on ionic liquids for advanced lithium polymer batteries, *Electrochimica Acta* 89 (2013) 823-831.

38. M. Ravi, Shenhua Song, Jingwei Wang, Reddeppa Nadimicherla, Zhongyi Zhang, Preparation and characterization of biodegradable poly(ϵ -caprolactone)-based gel polymer electrolyte films, *Ionics* 22 (2016) 661-670

39. Nilesh R. Chodankar, Deepak P. Dubal, Abhishek C. Lokhande, Chandrakant D. Lokhande, Ionically conducting PVA-LiClO₄ gel electrolyte for high performance flexible solid state supercapacitors, *J. Colloid and Inter. Science*, 460 (2015) 370-376.

40. Manoj K. Singh, Mohd Suleman, Yogesh Kumar, S.A. Hashmi, A novel

configuration of electric double layer capacitor with plastic crystal based gel polymer electrolyte and graphene nano-platelets as electrodes: A high rate performance, *Energy* 80 (2015) 465-473.

41. S. Nuur Syahidah, S.R. Majid, Super-capacitive electro-chemical performance of polymer blend gel polymer electrolyte (GPE) in carbon-based electric double-layer capacitors, *Electrochimica Acta* 112 (2013) 678-685.

42. Narendra Pal Singh Chauhan, Masoud Mozafari, Narendra Singh Chundawat, Kiran Meghwal, Rakshit Ameta, Suresh C. Ameta, High-performance supercapacitors based on polyaniline-graphene nanocomposites: Some approaches challenges and opportunities, *Journal of Industrial and Engineering Chemistry* 36 (2016) 13-29.

43. S. Nuur Syahidah, S.R. Majid, Ionic liquid-based polymer gel electrolytes for symmetric solid-state electric double layer capacitor operated at different operating voltages, *Electrochimica Acta* 175 (2015) 184-192.

44. Nitish Yadav, Kuldeep Mishra, S.A. Hashmi, Optimization of porous polymer electrolyte for quasi-solid state electrical double layer capacitors, *Electrochimica Acta* 235 (2017) 570-582.

45. Y. Kurma, G.P. Pandey, S.A. Hashmi, Gel polymer electrolyte based electrical double layer capacitors: comparative study with multiwalled carbon nanotubes and activated carbon electrodes, *J. Phys. Chem C* 116 (2012) 26118-26127.

46. Chiam-Wen Liew, S. Ramesh, A.K. Arof, characterization of ionic liquid added poly(vinyl alcohol)-based proton conducting polymer electrolytes and electrochemical studies on the supercapacitors, *Int. J. Hydrogen Energy* 40 (2015) 852-862.

47. Li Yang, Junyan Hu, Gang Lei, Hongtao Liu, Ionic liquid-gelled polyvinylidene fluoride/polyvinyl acetate polymer electrolyte for solid supercapacitor, Chemical Engineering Journal 258 (2014) 320-326.
48. Girum Ayalneh Tiruye, David Munoz-Torrero, Jesus Palma, Marc Anderson, REbeca Marcilla, Performance of solid state supercapacitors based on polymer electrolytes containing different ionic liquids, Journal of Power Sources 326 (2016) 560-568.

FIGURE CAPTIONS

Fig. 1. Photomacrograph of the 20 PVdF-HFP:80[PMpyr][NTf₂] gel polymer electrolyte film.

Fig. 2. (a) XRD pattern of MWCNTs, and their (b) low-magnification and (c) high-magnification TEM images.

Fig. 3. Schematic diagram of an EDLC along with an assembled EDLC supercapacitor.

Fig. 4. XRD patterns of PVdF-HFP + x [PMpyr][NTf₂] polymer electrolyte films (x = 0, 50, 60, 70 and 80 wt.%).

Fig. 5. TGA curves of pristine PVdF-HFP, 50PVdF-HFP:50[PMpyr][NTf₂] and 20PVdF-HFP:80[PMpyr][NTf₂] polymer films

Fig. 6. [PMpyr][NTf₂] concentration-dependent ionic conductivity of PVdF-HFP + x [PMpyr][NTf₂] gel polymer electrolyte films at room temperature.

Fig. 7. Cyclic voltammograms of PVdF-HFP + x [PMpyr][NTf₂] gel polymer electrolyte films at scan rate of 10 mV s⁻¹ (x = 50, 60, 70 and 80 wt.%).

Fig. 8. (a) CV curves of Cell-I and Cell-II at a scan rate of 10 mV s⁻¹; (b) and (c) cyclic voltammetry responses of Cell -I and Cell-II at different scan rates; and (d) specific capacitance of electrode for Cell -I and Cell-II as a function of scan rate.

Fig. 9. Electrochemical impedance plots of both EDLC cells at room temperature and its equivalent circuit is shown in inset.

Fig. 10. (a) Typical Galvanostatic charge-discharge curves of Cell-I and Cell-II in the first cycle (Current density = 5 mA cm⁻²); (b) and (c) charge-discharge curves of Cell-I and Cell-II at different cycles (current density = 5 mA cm⁻²); and (d) specific capacitance of electrode as a function of charge-discharge cycle.

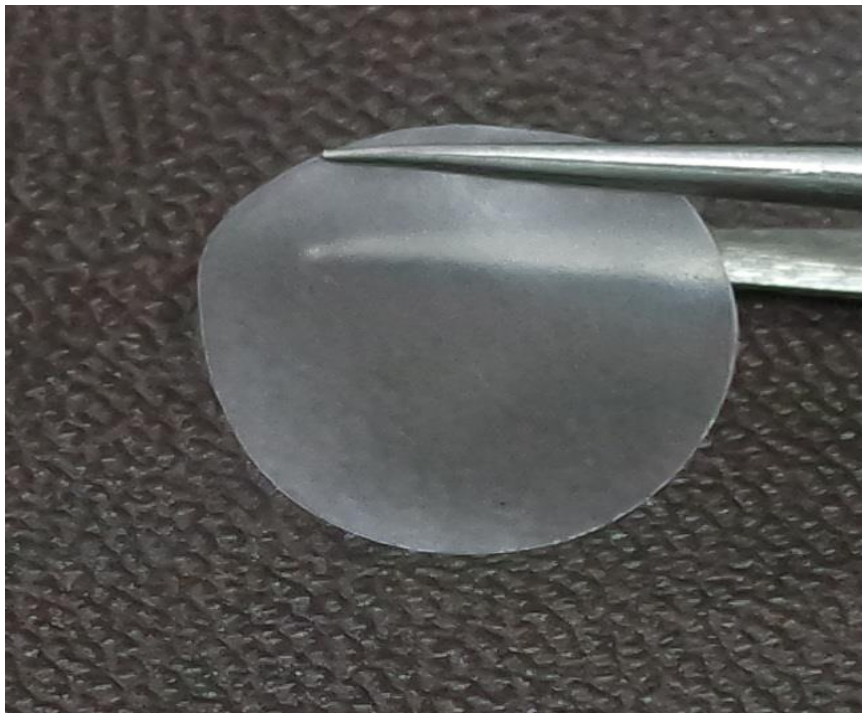
FIGURES

Fig. 1

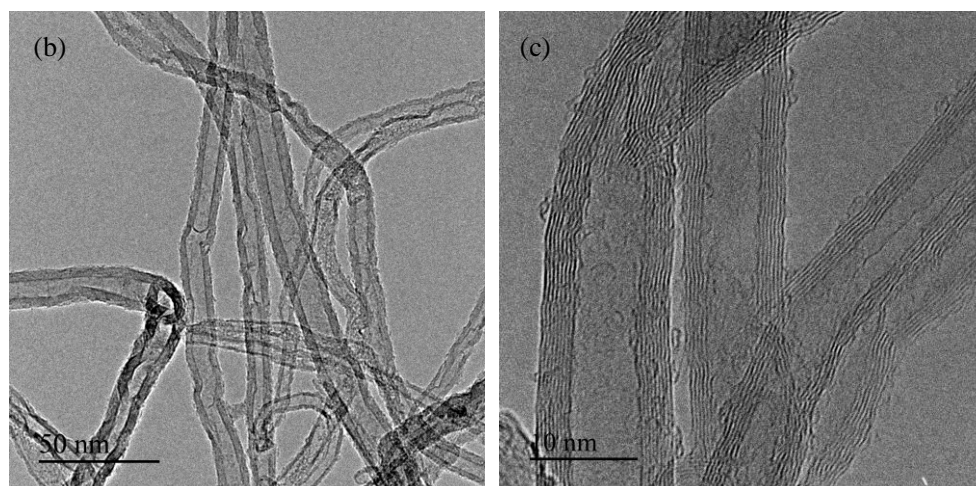
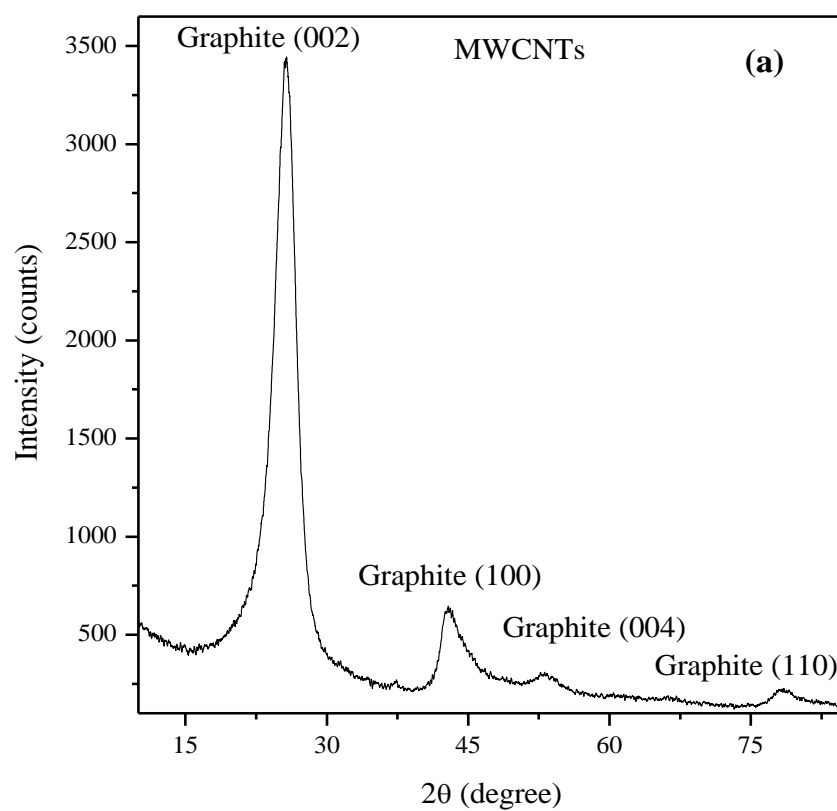


Fig. 2

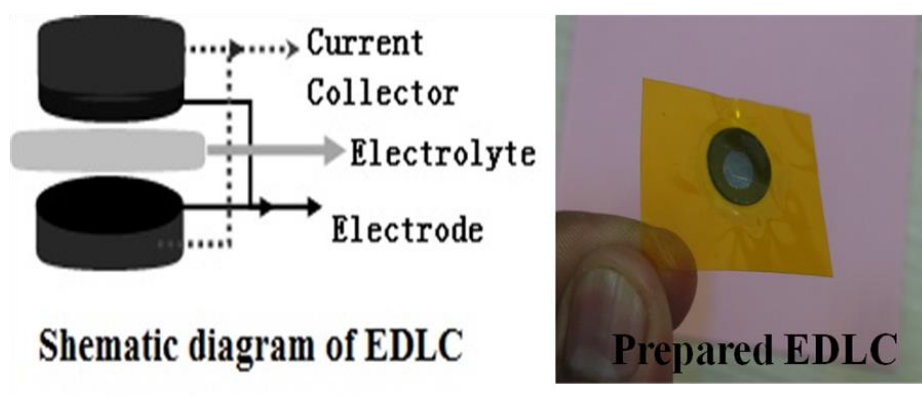


Fig. 3

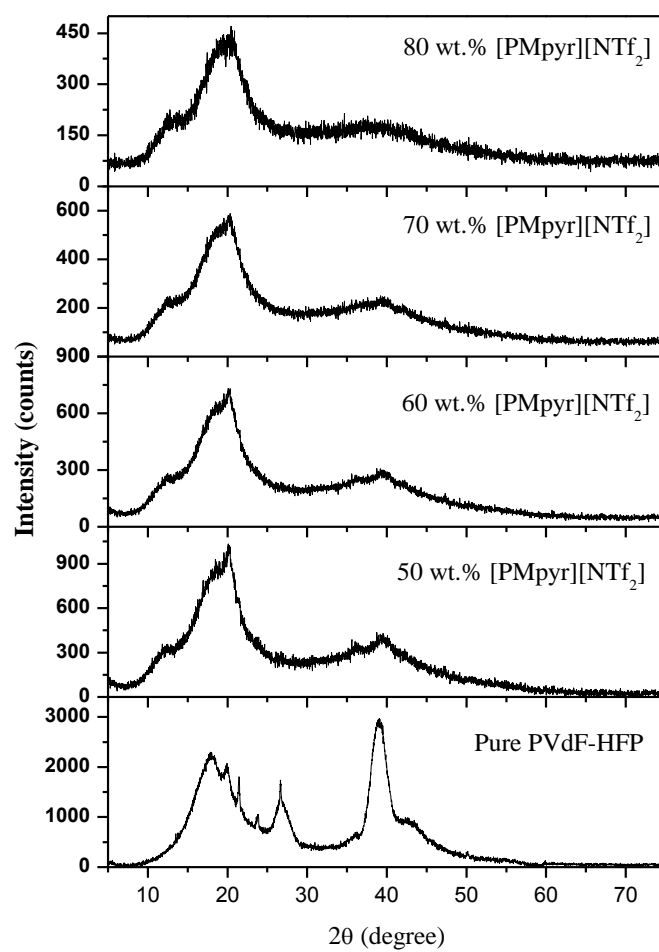


Fig. 4

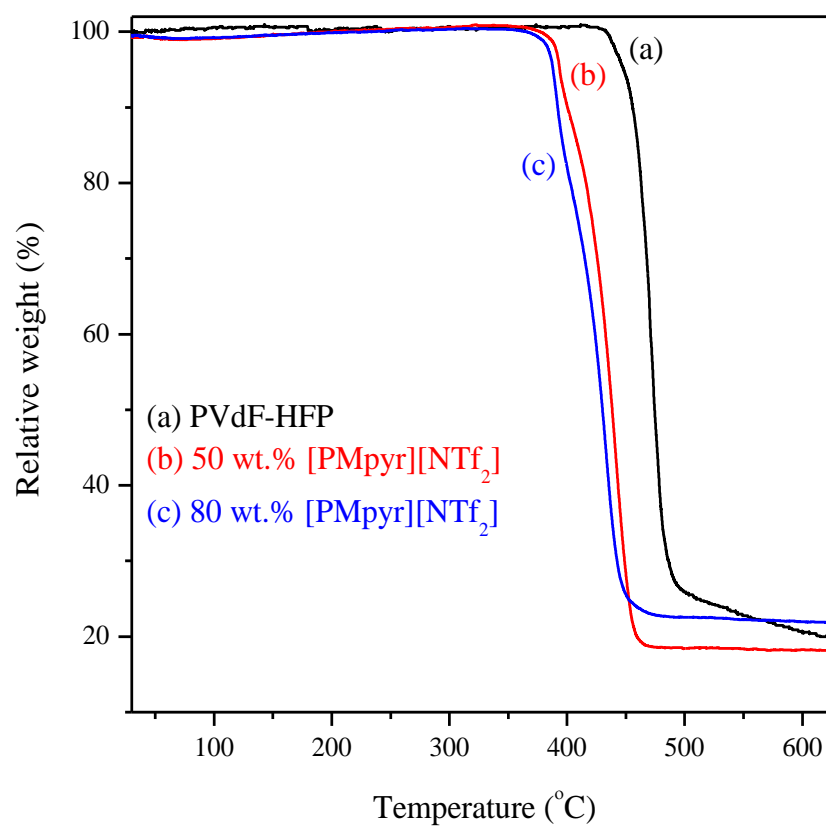


Fig. 5

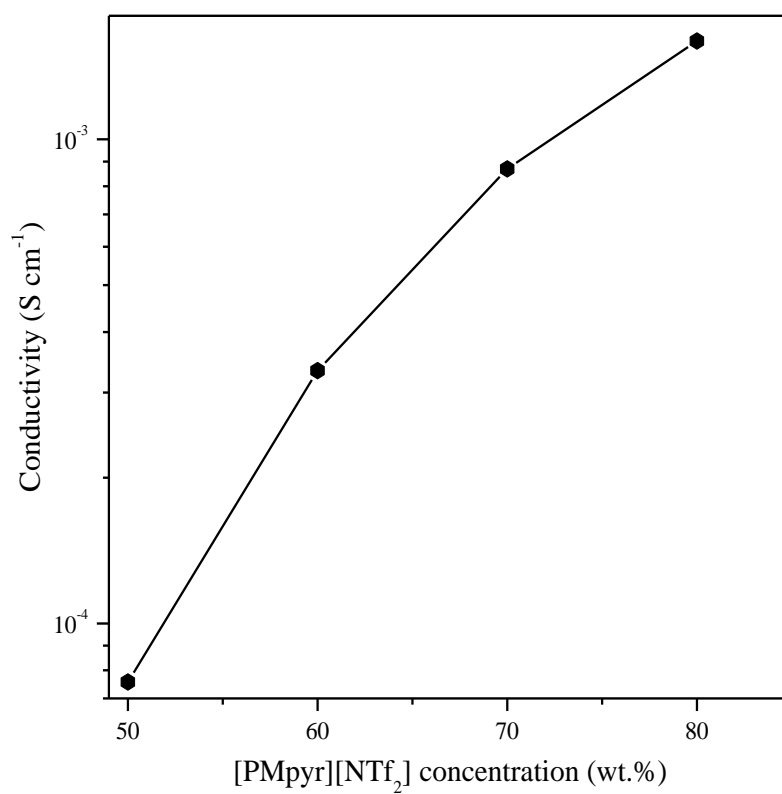


Fig. 6

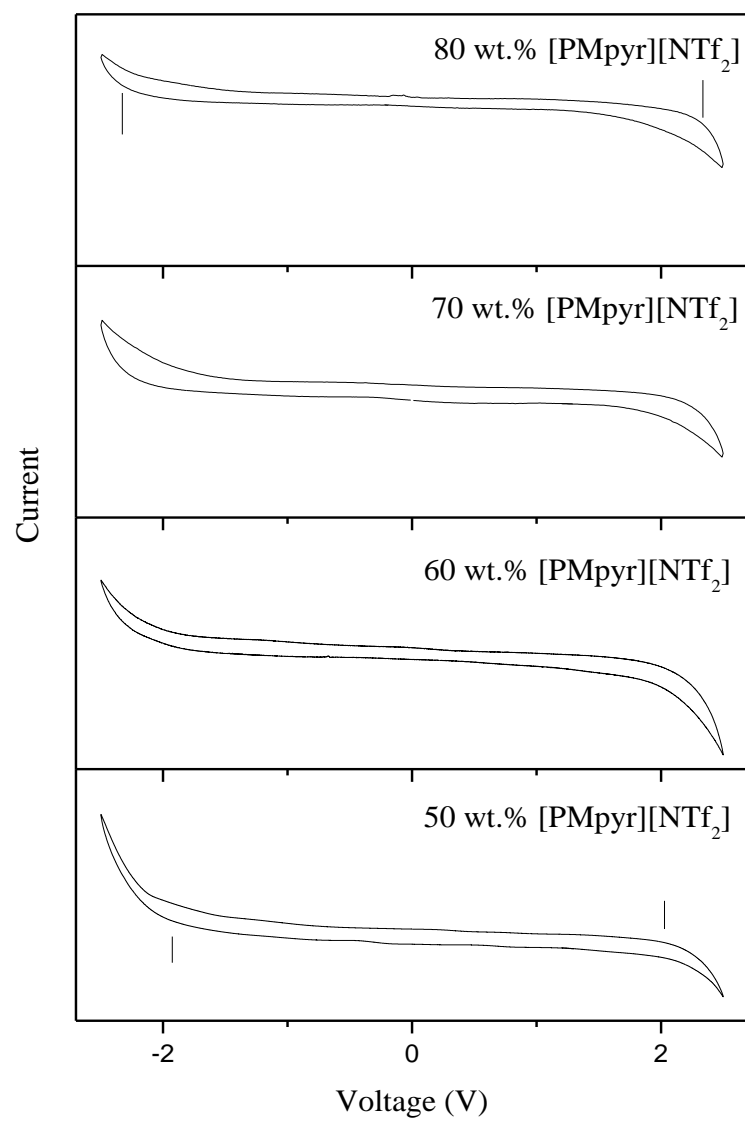
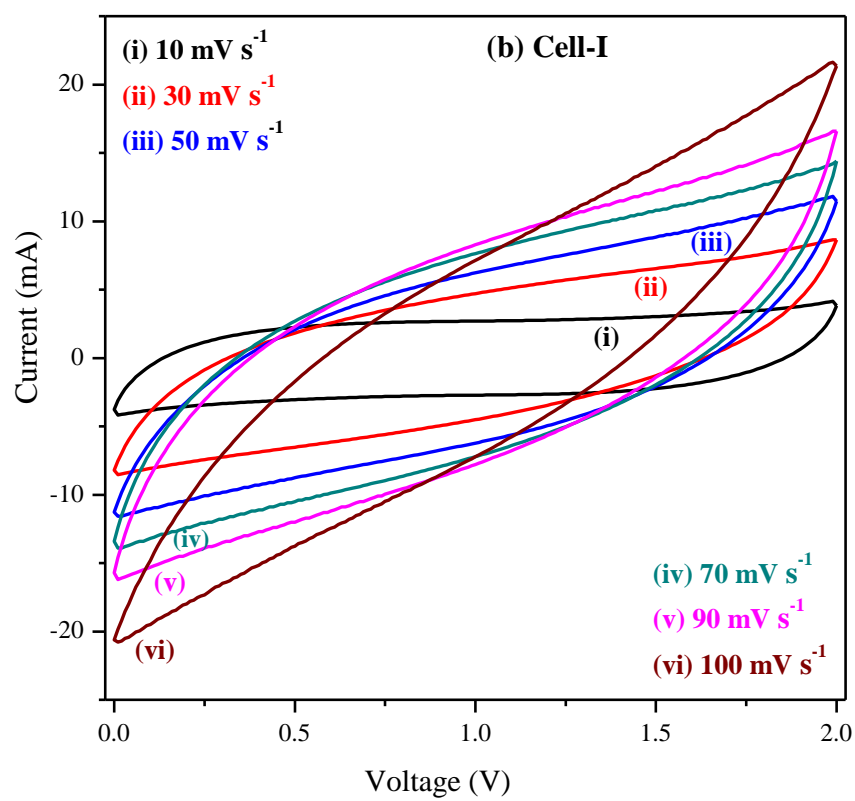
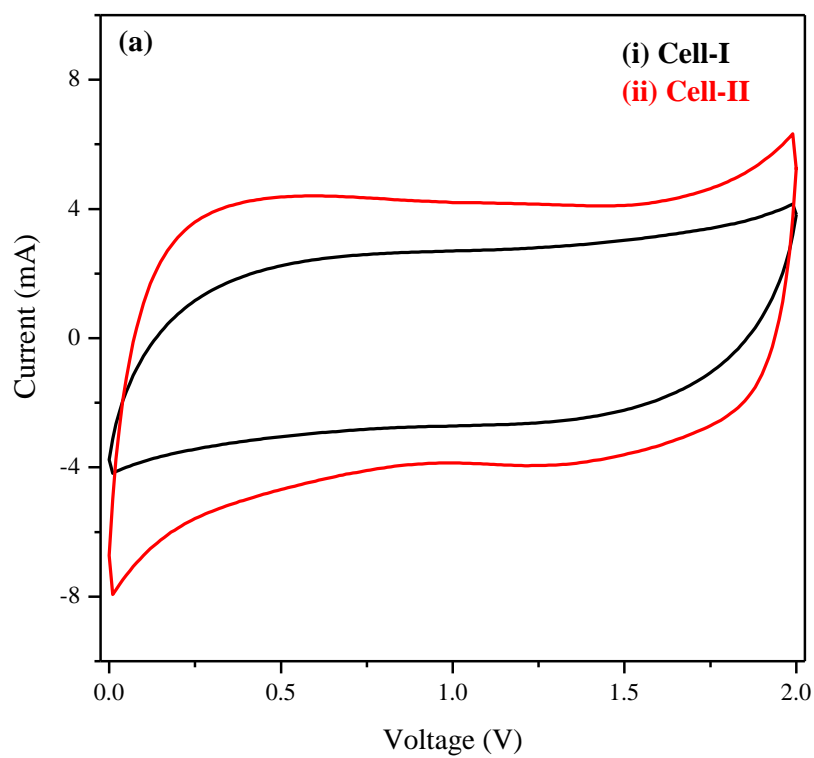


Fig. 7



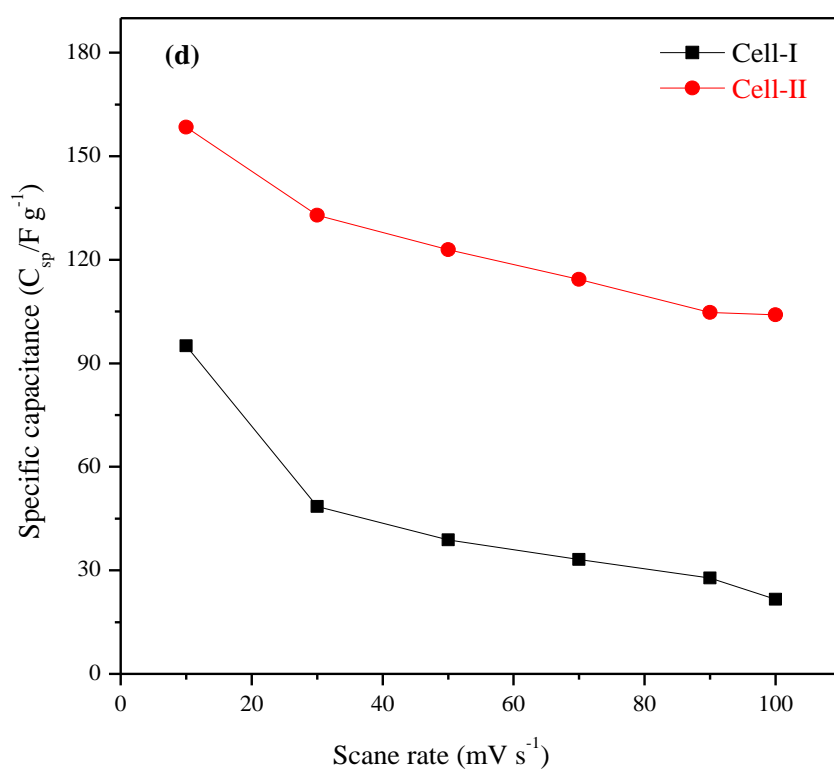
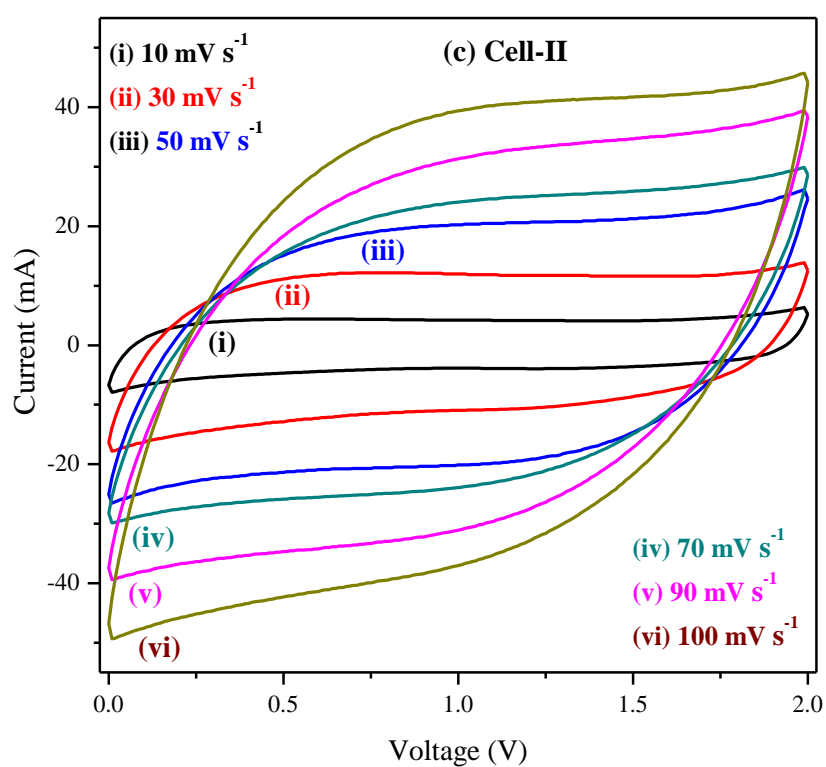


Fig.8

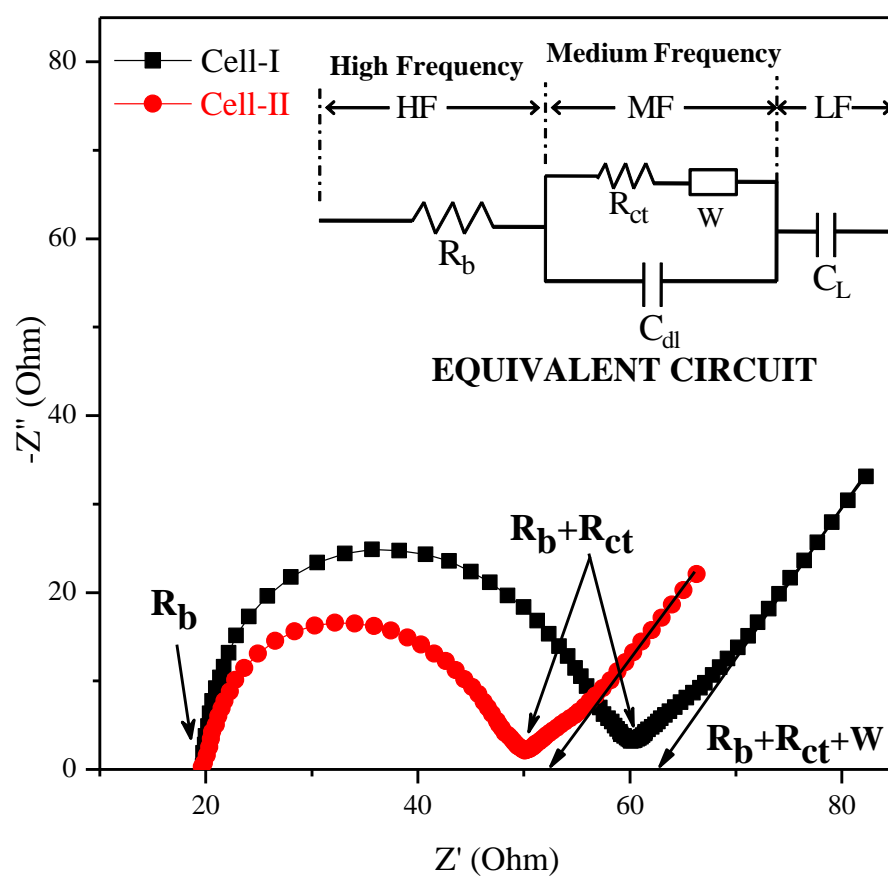


Fig. 9

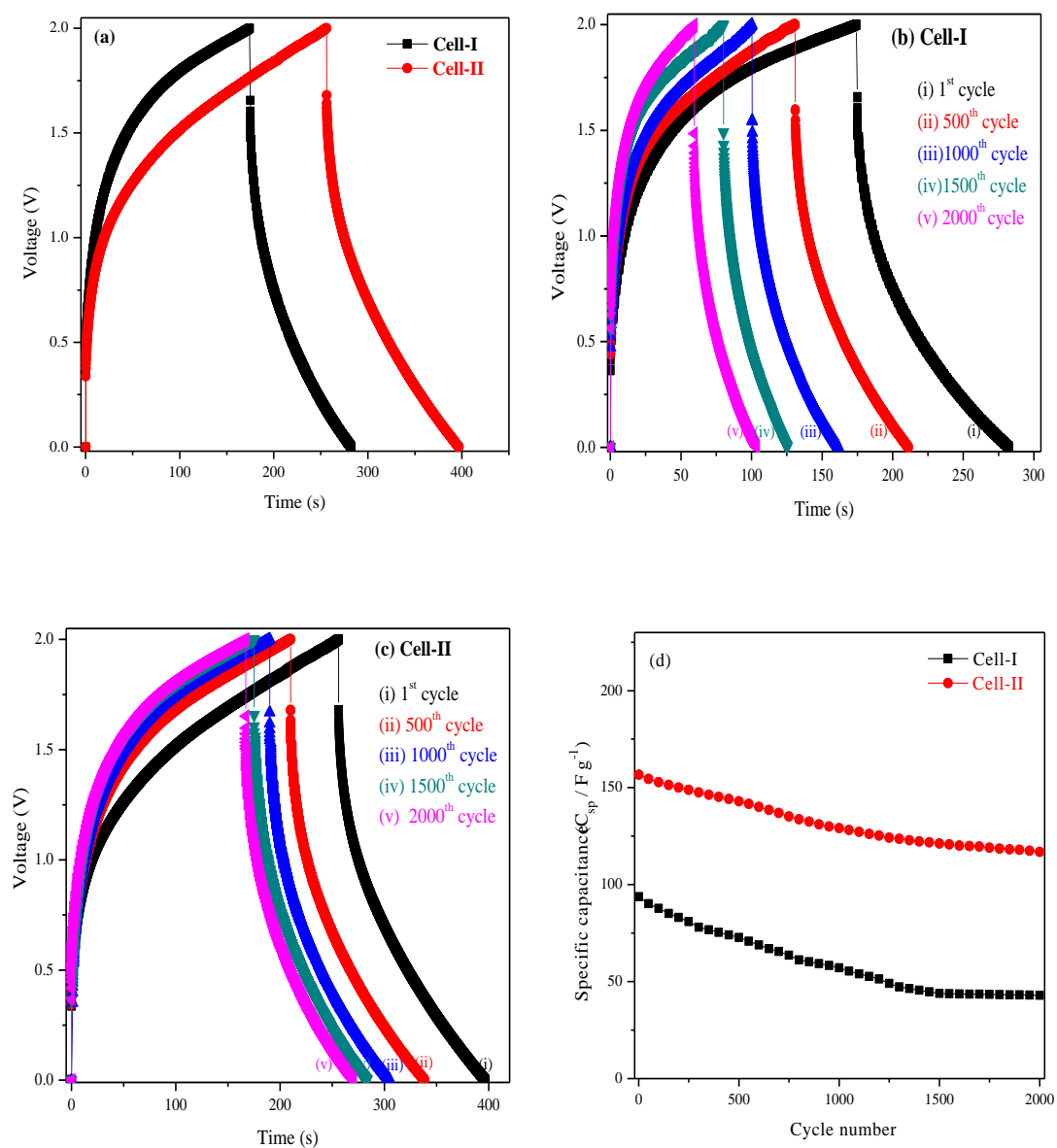


Fig. 10

Table 1. Comparison of specific capacitances of electrode between present gel polymer electrolyte-based EDLC supercapacitors and others

Electrode	Electrolyte	Specific capacitance (F g ⁻¹)
AC	PVdF/PVAc/BMIMBF ₄	93.3 [47]
Graphene	Polyacrylonitrile (PAN)/[BMIM][TFSI]	108 [21]
Porous carbon	PVP/PVdF-HFP/Mg(CF ₃ SO ₃) ₂ / [bdmim][BF ₄]	133 [41]
f-MWCNTs	PVdF-HFP/EMImFAP/LiPF ₆	127 [24]
Porous carbon	PVdF-HFP/MgTr	150 [43]
AC	PVdF-HFP/[PMpyr][NTf ₂]	93.72 [Present]
AC+MWCNT	PVdF-HFP/[PMpyr][NTf ₂]	156.64 [Present]

f-MWCNTs: Functionalized MWCNT;

Table 2. Typical charge-discharge characteristics of EDLCs in the first cycle at a constant current density of 5 mA cm⁻²

Sample	C _{sp} of electrode (F g ⁻¹)	Specific energy (Wh kg ⁻¹)	Specific power (kW kg ⁻¹)
Cell-I	93.72	17.86	2.88
Cell-II	156.64	30.69	4.13